High-speed and high accuracy IQE and L_{eff}-mapping – a tool for advanced quality control in the PV-industry

Th. Pernau, M. Spiegel, P. Fath, E.Bucher
Universität Konstanz, Fachbereich Physik, Fach X916, D-78457 Konstanz, Germany
Tel.: +49-7531-88-3644, Fax: +49-7531-88-3895

ABSTRACT. We present a fast LBIC system for the local (current-) analysis of photosensitive devices up to 20 cm x 20 cm in size. The system operates with four amplitude-modulated diode lasers (635 nm, 835 nm, 910 nm and 980 nm) coupled into one optical monomode-fibre. The fibre can be either attached to a galvanometer x-scanner system for fast measurements or to a microfocus optics allowing a minimum Gauss-shaped spot size of 5 µm FWHM for highly resolved measurements. The signal response is fed into four lock-in amplifiers, which demodulate the photocurrent or photovoltage at each of the four wavelengths. Another four lock-in amplifiers are used to record the spatially resolved reflection signal collected by reference solar cells. The reflection measurement is calibrated by scanning reflection standards of various reflectivities and surface roughness, depending on the type of solar cell to be analysed.
Keywords: Spectral response – 1: Reflection – 2: Lifetime – 3

1. INTRODUCTION

The **l**ight **b**eam **i**nduced **c**urrent (LBIC) technique is a spatially resolving characterisation method for any photosensitive device. The sample, i.e. a solar cell, is illuminated by a small light spot and the generated photocurrent is measured. By moving either the light spot or the sample, it is possible to record a current topography. With the development of advanced solar cell concepts, the LBIC scanning technique is very useful for solar cell process optimisation and monitoring.

2 EXPERIMENTAL SETUP

Unlike other LBIC systems [1, 2, 3, 4, 5, 6, 7], we have built up a 'dual mode' setup capable of either fast and less accurate or slow and accurate measurements.

2.1 Principle of operation

Fig. 1 shows the LBIC setup, called 'LBIC2000', as it was built up in the year 2000.

The core of the system is an 8-channel lock-in amplifier, whose four reference oscillators are used for the amplitude modulation of four laser diodes with the wavelengths 635 nm, 835 nm, 910 nm and 980 nm. The amplitude modulation of the lasers at different frequencies enables easy separation of the photocurrent components $I_{sc}(\lambda)$ using a current preamplifier and four channels of the lock-in amplifier. The other four channels are used to detect the reflection signal $R(\lambda)$ captured by the reflection measurement cells. Data values are stored after each line measured for safety. All relevant measurement parameters are stored

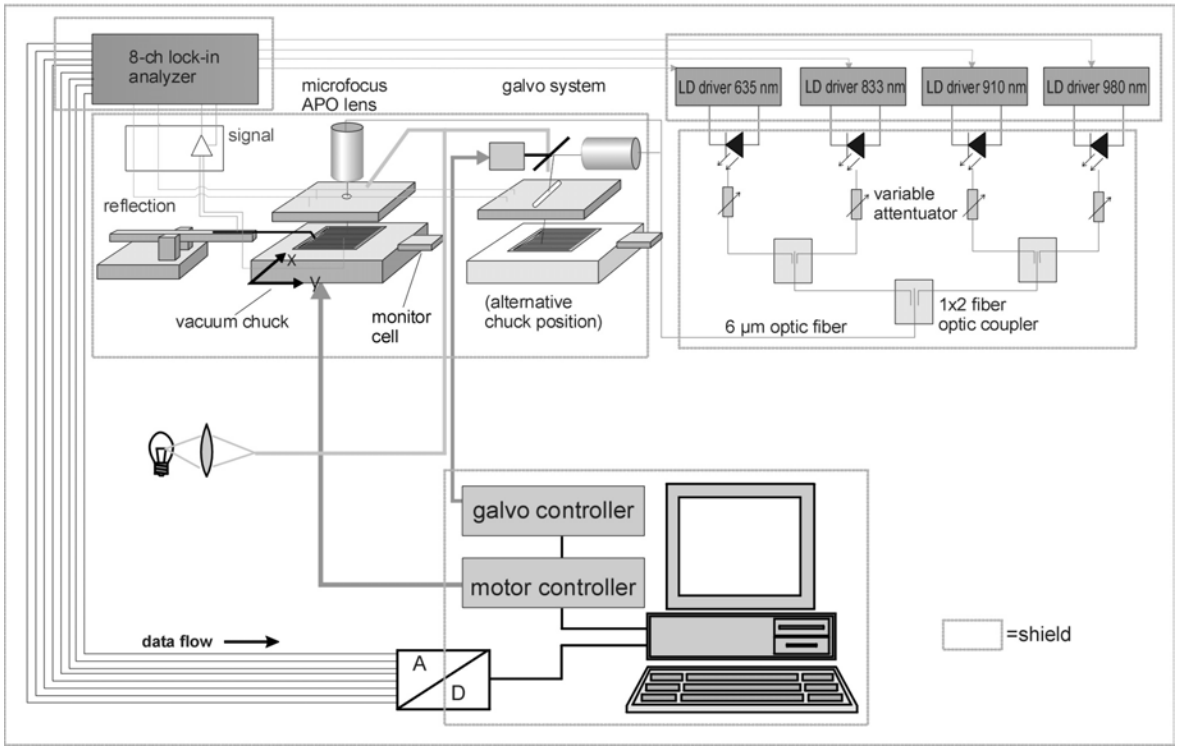

Fig. 1: schematic diagram of the UKN LBIC2000 system. The system can either perform fast measurements using the galvo optics or accurate measurements using the microfocus optics. The photocurrent at all four wavelengths is recorded parallel using a 8-channel lock-in amplifier.

in the header of the datafile. Bias light can be applied using a halogen lamp and a fluid lightguide (light transmission: 1400 nm ..400 nm).

1.2 Signal processing with the lock-in amplifier

The lock-in amplifier is a phase and frequency sensitive AC signal analyser which enables individual signal extraction out of a sum of AC signals, even if large DC offsets or noise are present. The operating principle is illustrated in Fig. 2.

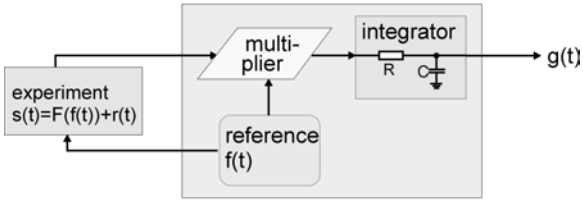

Fig. 2: Schematic of a one-phase lock-in amplifier. The signal s(t) is multiplied with the reference f(t) and integrated over a time span T_c, which is called the time constant of the lock-in amplifier.

The lock-in amplifier commonly has a built-in reference oscillator, which is generating the reference

$$f(t) = \sin(\omega_{ref} t) + A_o \quad (1)$$

A_o is an arbitrary offset, e.g. to operate a laser diode above the laser limit. The experiment is fed with the reference as input parameter. The reaction is a function of the reference plus noise (r(t)):

$$s(t) = F(f(t)) + r(t) \quad (2)$$

For further analysis, we have to look at the Taylor series of F(f(t)):

$$F(f(t)) = F(A_0) + \sin(\omega_{ref} t) \cdot F^{(1)}(A_0) + \frac{1}{2!}(\sin(\omega_{ref} t))^2 \cdot F^{(2)}(A_0) + ... \quad (3)$$

Where $F^{(i)}$ means $\frac{\partial^i F(f)}{\partial f^i}$

If the response of the experiment is linear, i.e. F(x)=B*x, then (3) reduces to:

$$F(f(t)) = B \cdot A_0 + B \cdot \sin(\omega_{ref} t + \varphi) \quad (4)$$

Note that φ is a phase shift between the signal component and the reference, caused by the experiment, cabling etc.

The multiplication followed by an integration in the lock-in amplifier corresponds to a correlation function:

$$g(t_0) = \frac{1}{T_c} \int_{t_0}^{t_0+T_c} f(t) \cdot s(t) dt \quad (5)$$

where t_o is the time when the readout is taken. The integral may be split into three parts:

$$g(t_0) = A_0 B \frac{1}{T_c} \underbrace{\int_{t_0}^{t_0+T_c} \sin(\omega_{ref} t) dt}_{0} + \frac{1}{T_c} \underbrace{\int_{t_0}^{t_0+T_c} r(t) \cdot \sin(\omega_{ref} t) dt}_{0} + \frac{B}{T_c} \int_{t_0}^{t_0+T_c} \sin(\omega_{ref} t) \cdot \sin(\omega_{ref} t + \varphi) dt \quad (6)$$

The first term which contains the offset is cancelled out if $T_c = \frac{n \cdot 2\pi}{\omega_{ref}}$ or if T_c is large enough, as the sine term is a symmetrical signal. The second term in (6) belongs to the random noise and is cancelled out under the same conditions as the first term, as the random noise times a symmetrical signal is also symmetrical. A 'practical' value for T_c is at least five times the reference oscillators period, the longer T_c the better. The last term of (6) is the interesting signal and computes to $\frac{1}{2} B \cos\varphi$. The lock-in amplifier usually delivers the quantity B without a factor. To obtain optimum signal, it is necessary to use a phase shifter to adjust φ=0°.
The dual phase lock-in amplifier does all that automatically, see Fig. 3.

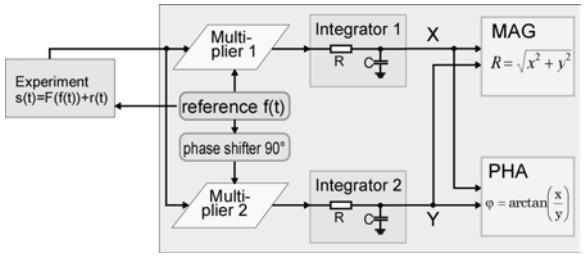

Fig. 3: The two-phase lock-in amplifier uses two one-phase lock-ins separated by a 90° phase shifter and generates a phase-independent readout.

The most advanced lock-in amplifier is the digital lock-in amplifier, which performs the operations described with a digital signal processor (DSP). This enables more complex signal retrieving operations, e.g. synchronisation of the time constant with the reference oscillator and digital external reference tracking. This allows the reduction of the integration time down to one single reference period. The only noise the digital lock-in produces is the quantisation noise of it's A/D-converter.

1.3 Analysing multiple AC signals with the lock-in amplifier

The LBIC2000 system operates with four lasers in parallel, i.e. the signal contains four AC components with different modulation frequencies:

$$s(t) = offset + r(t) + B_1 \sin(\omega_1 t) + B_2 \sin(\omega_2 t) + B_3 \sin(\omega_3 t) + B_4 \sin(\omega_4 t) \quad (7)$$

Then the product s(t)*f(t) contains interference terms, e.g. interference between ω_1 and the other three frequencies:

$$interf.1 = \sin(\omega_1 t) \cdot (B_2 \sin(\omega_2 t + \varphi_2) + B_3 \sin(\omega_3 t + \varphi_3) + B_4 \sin(\omega_4 t + \varphi_4)) \quad (8)$$

When integrating over the interference terms, the most relevant component is the term with the lowest interference frequency. Once again, the integration time constant should at least be longer than 5 times the interference period in order to cancel out the interferences. The interference frequency or period of two sinusoidal components is governed by their frequency spacing. In the LBIC2000 system the frequency spacing is around 200 Hz, so that the minimum time constant T_c should be 25 ms. For fast measurements a time constant of 30 ms is used, whereas for accurate measurements T_c is set to 100 ms. It is even possible to use only 10 ms time constant for rather noisy and fast measurements. The reference frequencies of the LBIC2000 system are between 700 and 1300 Hz, therefore if operating only at one wavelength, a time constant of only 5 ms is enough. For industrial size solar cells (12.5 x 12.5 cm² or larger), the reference frequency should not exceed 2 kHz due to capacitance effects. Furthermore, not all current preamplifiers are capable of driving high capacitive loads and operating against DC offsets.

1.4 Optics and reflection measurement

All lasers are coupled into a 5 µm step index monomode optical fibre using Y beamsplitters. The optical attentuators allow power adaption to the nonuniform coupling efficiency of the beamsplitters.

For accurate measurements, the optical fibre is attached to a microfocus optic enabling spot sizes down to 5 µm FWHM. The microfocus optic is directly attached to a punctured reflection measurement cell. The reflection measurement is not omnidirectional, therefore the reflection calibration standard and the sample to be tested must be comparable in surface roughness. Further error correction can be performed with the LBIC evaluation software.

For fast measurements, the optical fiber may be connected to a galvanometer linescanner. The working distance from the galvanometer optic to the sample is 250 mm and the spot size is 120 µm FWHM. The advantage of the linescanner is that it shows no geometric distortion, whereas a standard xy-galvo scanner shows a pincushion distortion depending on the deflection angle. This may be corrected by sophisticated motorised adaptive optics, which is at least as expensive as the rest of the LBIC system. By doing only linescanning with the galvo system, there is still the possibility to record reflection data using a reflection measurement cell with a slit to let deflected beam pass through. Once again, the reflection measurement is not omnidirectional. The reflection data shows distortions due to the contact grid of the reflection measurement cell, as the galvo scanner moves the light beam with respect to the reflection measurement cell. This is however acceptable since grid line width is only 100µm, which is below the stepsize commonly used for fast measurements.

1.5 Scanning and motor controls

Scanning action is controlled via a computer. In high accuracy mode, the sample is moved by the x/y tables with respect to the microfocus optics. The x/y tables resolve 0.5 µm. It is reasonable to perform scans at step sizes below the optics resolution for the same reason as the human eye can see stars even below its angular resolution. If the object to be detected is smaller than the spot size, its detection limit is governed by the point-to-point S/N-ratio. If e.g. a signal change of 5% F.S. can surely be resolved, the minimum detectable object size is 0.25 times the spot size. In the LBIC2000 system, we managed to reduce the point-to-point noise even below 0.4 %, so that a step size of 1 µm to investigate some details makes sense.

The fast and less accurate scanning is done by a combination of the x-scanning via galvanometer and the y-scanning with the motorised table. The galvanometer scanner is up to 100 times faster than the motorised table, since only a little mass is moved. This saves a lot of time when doing the line scanning in x-direction. For the row scanning in y-direction (which is done only at the end of each line), the galvanometer scanner has no advantage.

1.6 Calibration and stability

Laser power $P(\lambda)$ is controlled by a monitor cell, which is attached to the sample chuck. The motorised tables can resume calibration position at any time before, during and after the LBIC scanning action. Additionally, all laser diode drivers are running in 'constant power' mode controlled by the lasers built-in photodiode. The long term stability of the LBIC system is better than 1,3 % in 24 hrs. This is achieved by temperature control of lasers as well as sample cabinet.

2. EXPERIMENTS

3.1 High accuracy measurements

LBIC is useful in any case where fine details have to be investigated. With a maximum resolution of 2000x2000 points, we can resolve 10 µm on a 2x2 cm² solar cell.

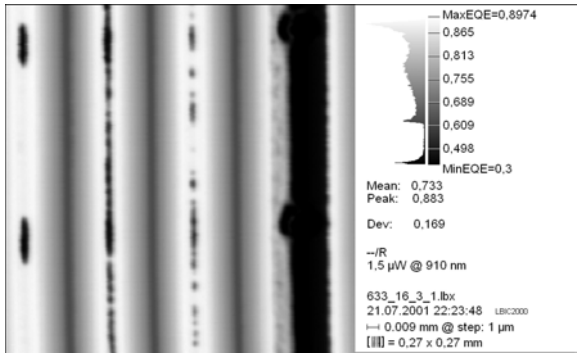

Fig. 4: LBIC-scan of a V-textured monocrystalline solar cell. The shadowed regions are the grooves. On top of the ridges, there are remainders of the galvanic metallisation which are not clearly visible with the optical microscope since it does not analyse the photocurrent. This map was recorded with a stepsize of 1 µm.

3.2 Quick measurements

When reduced image quality is acceptable, an LBIC map recording time of a few minutes is enough to get useful information: The map in Fig. 5 took 11 min for recording. The measurement was done using the galvanometer scanner with a stepsize of 1 mm and a time constant of 30 ms.

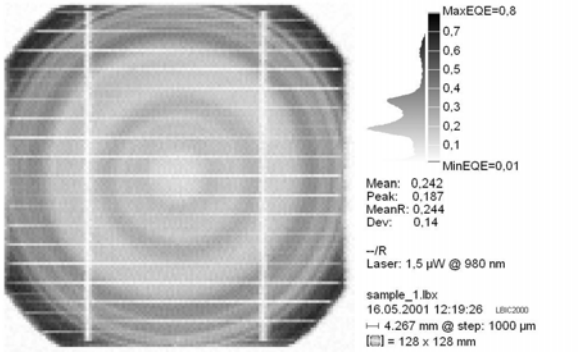

Fig. 5: Fringes caused by oxygen induced stacking faults (OSF) on a 12.5 x 12.5 cm² CZ solar cell. The OSF reduce diffusion length and are best visible using a long detection wavelength, here: 980nm.

3.3 Calculation of L_{eff}-maps

When recording short circuit current I_{sc} and reflection R at various wavelength in the near IR (750 nm ... 1100 nm), it is possible to calculate a map of the effective diffusion length L_{eff} using the formula [8]:

$$(9) \quad \frac{1}{IQE} = 1 + \frac{1}{\alpha L_{eff}}$$

α is the penetration depth depending on the wavelength of the incident light, the internal quantum efficiency IQE computes from the short circuit current, incident light and the reflection:

$$(10) \quad IQE(\lambda) = \frac{I_{sc}(\lambda)}{P(\lambda)} \cdot \frac{hc}{e\lambda} \cdot \frac{1}{1 - R(\lambda)}$$

The fitting algorithm for extraction of L_{eff} according to (9) is simple and stable, however the results should be critically investigated [9]. The evaluation of the IQE of thin (<250 µm) solar cells with good surface and back side passivation tends to deliver too high L_{eff}-values. The improved approximation for L_{eff} analysis includes the bulk diffusion length L_{bulk} [10]:

$$(11) \quad IQE = \frac{1 - \frac{1}{\alpha L_{eff}}}{1 - \frac{1}{\alpha^2 L_{bulk}^2}}$$

This however is less easy to be fitted. At the moment, our fitting algorithm is not stable enough to cope with the increased point-to-point noise in the galvanometer scanning setup.

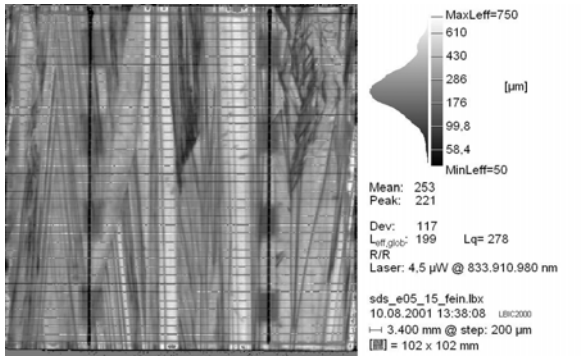

Fig. 6: L_{eff}-map of a 10x10 cm² EFG solar cell with aluminum BSF and ARC made of PECVD silicon nitride. The hydrogen released from the PECVD SiN causes a good bulk passivation, as can be seen form locally high L_{eff}-values.

3. CONCLUSION

LBIC is an excellent tool to investigate spatially distributed current generation of a solar cell. Many interesting, disturbing or even deteriorating properties of individual solar cells can be revealed by an LBIC measurement. With a specially designed LBIC system, current detection at multiple wavelengths gives additional information 'in depth'. It is possible to acquire 400 and more data points per second, so that LBIC maps of reasonable quality can be recorded in less than half an hour.

4. ACKNOWLEDGEMENTS

This work was supported by the E.C. within the Fast-IQ project under contract No. ERK6-CT1999_00002. We would like to thank the project partners for the fruitful discussions as well as the exchange of measurement data and samples.

REFERENCES

[1] M. Acciarri et al., Mater. Sci. Eng., B42 (1996) 208.
[2] G. Agostinelli et al., Proceedings of the 2nd WCPEC, Vienna, Austria, 1998, p. 184.
[3] G. Agostinelli, G. Friesen, F. Merli, E. Dunlop, M. Acciarri, A. Racz, J. Hylton, R. Einhaus, T. Lauinger, '*Large Area Fast LBIC as a Tool for Inline PV Modula and String Characterisation',* OA 1.2, this conference
[4] M. Stemmer, Appl. Surf Sci. **63** (1993), 213-217
[5] J. Carstensen, G. Popkirov, J. Bahr, H. Föll, Proc.16th EPSEC, Vol. II, p. 1627-1630
[6] J. Bajaj, L.O. Bubulac, P.R. Newman, W.E. Tennant, J. Vc. Sci. Technol. A 5(5), Sept/oct 1987, 3186-3189
[7] W. Warta et al., Proc. 2nd WCEPSEC, Wien, 1650 (1998)
[8] P.A. Basore, IEEE Trans. Electron Devices vol. 37 (1990), p.337
[9] S. Keller et al., IEEE Trans. Electron Devices vol. 45 (1998), p. 1569
[10] M. Spiegel et al, Proceedings of the 28th IEEE PVSC, Anchorage, Alaska, 2000.